Hindawi Publishing Corporation
Journal of Nanomaterials
Volume 2011, Article ID 473629, 12 pages
doi:10.1155/2011/473629

Research Article

Mechanism and Growth of Flexible ZnO Nanostructure Arrays in a Facile Controlled Way

Yangping Sheng, Yang Jiang, Xinzheng Lan, Chun Wang, Shanying Li, Xinmei Liu, and Honghai Zhong

School of Materials Science and Engineering, Hefei University of Technology, Hefei, Anhui 230009, China

Correspondence should be addressed to Yang Jiang, apjiang2002@yahoo.com

Received 8 April 2010; Accepted 26 May 2010

Academic Editor: Quanqin Dai

Nanostructure arrays-based flexible devices have revolutionary impacts on the application of traditional semiconductor devices. Here, a one-step method to synthesize flexible ZnO nanostructure arrays on Zn-plated flexible substrate in $Zn(NO_3)_2/NH_3 \cdot H_2O$ solution system at 70–90°C was developed. We found out that the decomposition of $Zn(OH)_2$ precipitations, formed in lower $NH_3 \cdot H_2O$ concentration, in the bulk solution facilitates the formation of flower-like structure. In higher temperature, 90°C, ZnO nanoplate arrays were synthesized by the hydrolysis of zinc hydroxide. Highly dense ZnO nanoparticale layer formed by the reaction of $NH_3 \cdot H_2O$ with Zn plating layer in the initial self-seed process could improve the vertical alignment of the nanowires arrays. The diameter of ZnO nanowire arrays, from 200 nm to 60 nm, could be effectively controlled by changing the stability of $Zn(NH_3)_4^{2+}$ complex ions by varying the ratio of $Zn(NO_3)_2$ to $NH_3 \cdot H_2O$ which further influence the release rate of Zn^{2+} ions. This is also conformed by different amounts of the Zn vacancy as determined by different UV emissions of the PL spectra in the range of 380–403 nm.

1. Introduction

Flexible devices based on inorganic materials are beginning to show great promises for technical or commercial interests [1–3]. And in situ fabricating of inorganic materials from flexible substrate will promote the development of flexible devices [4]. Among the inorganic materials, ZnO is one of the most important wide-band-gap semiconducting materials due to optoelectronic, catalytic, lasing, electrical, and piezoelectric properties [5–7]. ZnO nanowire arrays have been broadly investigated because of their applications in solar cells [8–10], sensors [11–13], lasers [14], light-emitting diodes [15, 16], and so on [17–19]. Various physical [20–22], chemical [23–32], and electrochemical methods [33–36] have been developed to synthesize ZnO nanowire arrays. Among these methods, physical methods like thermal evaporation involve complex procedures, sophisticated equipment, and relative high temperature. In contrast, chemical methods, also called solution methods, have advantages in their easy procedures, simple equipment, and low temperature. Meanwhile, solution methods for preparing ZnO nanowire arrays have appealing potential for scale-up to meet the needs of industrial applications.

The generally employed solution methods reported are seeded growth on ZnO nanoparticles or film-coated substrates [37, 38]. Aligned ZnO nanowire arrays can be synthesized via a two-step process. The first step is formation of a ZnO-seeded layer by pretreated methods [24, 31, 32, 37, 38] or self-seeded technology [39]. Textured ZnO nanocrystal and ZnO thin film have been successfully demonstrated to produce large-scale ZnO nanowire arrays [24, 37, 38]. The next step is solution growth by controlling the supersaturation of the solution, through the formation of Zn^{2+} complex, to retard the homogeneous nucleation in bulk solution and promote the heterogeneous nucleation onto the seeded layer [40, 41]. However, the coatings of seed layer are complex and are difficult to reproduce [42]. For self-seeded technology, seeded layers are formed onto

the substrates from the solution in the initial growth stage which do not need any pretreatment of the substrates. And the ZnO nanowire arrays can be directly fabricated onto the substrate without pretreatment. The choices of substrates, however, are also limited by the phase match between the substrates and the ZnO nanowire arrays. Only some substrates with good phase match properties can be used [39, 43, 44]. The development of flexible devices needs novel synthesis methods of direct growth of ZnO nanoarrays onto the flexible substrates with broad choices. Therefore, ZnO nanowire or other nanostructure arrays grown on various substrates in large-scale low-cost way with high reproducibility is still challenging.

Plating technologies can be applied to various substrates, that is, polymer substrates by metalizing process, flexible metal substrates [45, 46]. And the plating layer generally has good contact with the substrate, which can guarantee the stability of device performance. There have been already some reports on fabricating ZnO nanostructures from Zn foil [43, 47–50]. If Zn foil can be replaced with Zn plating layer, the growth of ZnO nanowire arrays could be extended to various substrates, not Zn foil only. Meanwhile, the electric conductive property of the Zn plating layer can meet the needs of the electrical contact with the substrates in the applications of devices. In this work, by combining the Zn plating technology and solution methods, ZnO nanowire arrays were successfully fabricated from the Zn plating layer on the flexible copper foils, which are highly conductive and have not been used as substrate for ZnO nanowire arrays. The prepared ZnO nanostructures have good contact with the substrates. The morphology of the Zn plating layer was found to have little effect on the growth of ZnO nanowire arrays. By controlling the growth parameters like concentrations of $NH_3 \cdot H_2O$ and Zn^{2+} ions and growth temperature, well-aligned ZnO nanowire arrays, nanoplate arrays, and flower-like structure can be achieved, and the aspect ratio, density, and alignment of ZnO nanowires arrays can also be turned. Photoluminescence measurements were conducted to investigate the optical properties of the synthesized ZnO nanostructures, and they were determined by solution growth conditions. Zn plating technology has been maturely employed in industry and can been applied to various substrates. Thus this method is easy to scale up and applicable to various other substrates.

2. Experimental Sections

All chemicals were purchased from Shanghai Chemical Reagent Co, Ltd, and used as received without further purification.

2.1. Zn Plating. Zinc plating was performed according to [51] with some modification. Nickel, stainless, and copper foils were used for demonstration as flexible substrates. The plating bath was composed of $ZnCl_2$ (65 g/L), KCl (190 g/L), and H_3BO_3 (25 g/L), and pH was adjusted to 5 by 1 M hydrochloric acid. A piece of copper foil (2 cm×4 cm×1 mm) was used as cathode substrate and Zn foil as anode. The plating was performed under a constant current density of 20 mA/cm^2, temperature 25°C for 0.5–1 h. A white layer of Zn was covering the flexible substrates. Here, copper foils were used for experiment convenience.

2.2. ZnO Nanostructures Growth Procedures. The syntheses were performed in a 50 ml pyrex glass bottle with a screw cap. $Zn(NO_3)_2$ was prepared to 0.03 M aqueous solution, and a certain amount of ammonia (0.1 g, 1 g) (85 wt%) was slowly added. With several minutes stirring, Zn-plated copper foil was suspended upside down in the solution. Then the bottle was sealed and heated at 80°C for 12 h. After growth, the substrate was removed from the solution, rinsed with deionized water, and then dried at 60°C for 6 hours. The white Zn plating layer was changed into a gray layer of ZnO.

The crystal structure analysis was carried out by powder X-ray diffraction (XRD) using Cu K_α radiation at room temperature. The morphologies of the ZnO nanostructure were researched by field emission scanning electron microscopy (FESEM) with accelerating voltage of 5 KV in Sirion200 (FEI,10KV) and energy dispersive X-ray spectroscopy (EDX). Room temperature photoluminescence (PL) spectra were recorded on a JY-Labram spectrometer with a continuous wave He-Cd laser focused at ~2 μm as the exciting source at 325 nm.

3. Results and Discussion

The surface morphology of the Zn layer electroplated on the copper foil is shown in Figure 1. In Figure 1(a), we can see that the Zn plating layer is a continuous film and is composed of hexagonal platelets. In higher magnification, scale bar 500 nm, as shown in the inset picture of Figure 1(a), the Zn grain is highly crystalline and has smooth grain surface. This can be conformed by XRD pattern, as shown in Figure 1(b). All the peaks can be indexed to Hexagonal Zn (JCPDS Card NO. 04-0831, space group P63/mmc) and the substrate cubic Cu (JCPDS Card NO. 04-0836, space group Fm3m). The (101) peak of Zn and (111) peak of Cu are very close, thus it is hard to distinguish those two peaks. The influences of Zn plating layer will be discussed later in mechanism section.

Figure 2(a) illustrates the low magnification SEM image of ZnO nanowire arrays grown on the Zn-plated Cu foil with using 1 g $NH_3 \cdot H_2O$ at 80°C for 10 hours. It can be seen that ZnO nanowire arrays grow normal to the Cu substrate with fine alignment. The optical image of the arrays on the flexible Cu foil is illustrated on the inset of Figure 2(c). It shows that as-prepared ZnO nanowires arrays are grey and cover well the flexible Cu foil. The pattern of nanowire arrays is also affected by the surface morphology of the Zn plating layer. As shown in Figure 1(a), the surface of Zn plating layer is not smooth, with some hill-like protrusion morphology. Thus, the ZnO nanowire arrays are not uniformly covered on the Cu foil but duplicate the topography of Zn plating layer. However, the nanowire arrays vertically rise from the Zn layer as shown in higher magnification in Figures 2(b) and 2(c). Note that, with this method to produce nanowire arrays, the quality of the arrays is not affected by the roughness of the

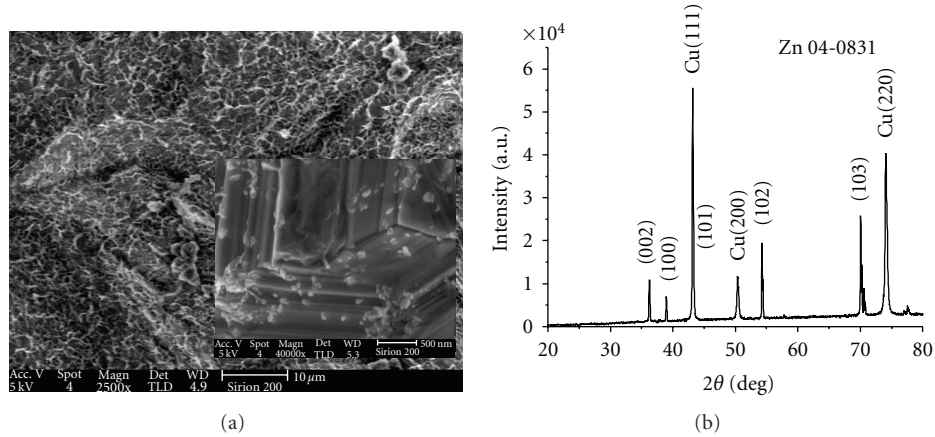

Figure 1: (a) SEM image of Zn plating layer; the scale bar is 10 μm. The inset is a higher magnification image with scale bar 500 nm. (b) XRD pattern of Zn-plated copper foil.

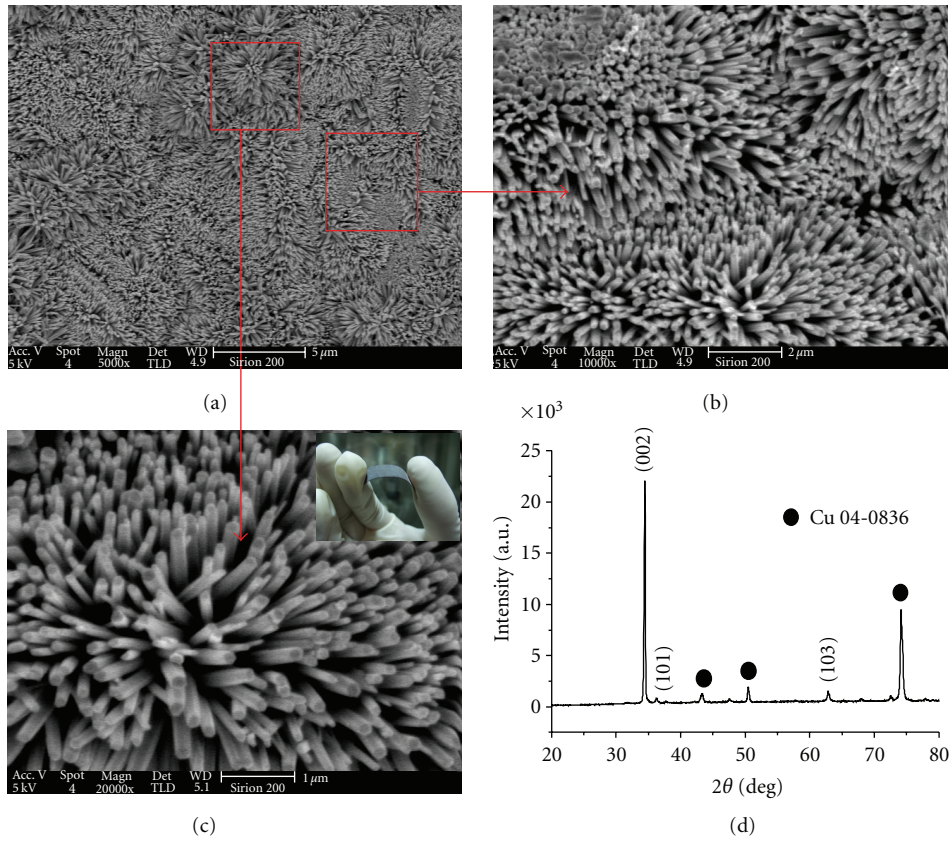

Figure 2: SEM images of ZnO nanowire arrays. Scale bar of (a) is 5 μm, (b) 2 μm, and (c) 1 μm. (d) XRD pattern of the ZnO nanowire arrays on the copper foil. The inset of (c) is the photograph of the ZnO nanowire arrays on the flexible copper foil.

plating layer. Meanwhile, designing the topography of the plating layer rationally may open a new economic way to pattern the nanowire arrays which may have 3-dimensional distribution [45, 46]. From Figures 2(b) and 2(c), we can clearly see the good orientation of the arrays and that single ZnO nanowires have smooth surface and average diameters of 130 nm. In addition, to investigate the contact between the ZnO nanowire arrays and substrate, ultrasonic treatment was performed. After two minutes of treatment, the ZnO nanowire arrays were still adhered to the substrate tightly; no peel off was observed. This means good contact properties to the substrate, which would have obvious advantages in device fabrication.

The crystallinity of the ZnO nanowire arrays is also investigated by the XRD methods. In Figure 2(d), the XRD patterns of the ZnO nanowire arrays grown on the Zn-plated

Cu foil were show. The peaks marked with solid circles are assigned to the cubic copper (JCPDS Card NO. 04-0836, space group Fm3m). These peaks are from the copper substrate. The rest of the peaks are in agreement with the typical wurtzite structure of ZnO diffraction pattern (JCPDS Card NO. 36-1451, space group $P6_3mc$). The sharp (002) peak of the ZnO nanowire indicates good crystallinity, and favorable growth direction of ZnO crystals is (002). As reported in other literatures [52], the extrastrong (002) reflections of the ZnO nanowire also indicate good alignment of the nanoarrays. The disappearing of the reflections of Zn layer indicated that the Zn layer reacted with solution completely.

The growth of ZnO nanowire arrays is a complex way and mostly considered to be a process including the formation of a ZnO seed layer and subsequent growth of crystal. Many researches have suggested that the quality of seed layer influences the alignment and density of the ZnO nanowire arrays [53, 54]. In the first seed layer step, preseed texture layer was generally employed by most synthesis routes [23–32, 37, 38]. The self-seed method in which a seed layer is formed preceding the crystal growth during the solution reaction is a more competitive way. The preparation of ZnO nanowire arrays based on Zn metal powder or layer has been reported to be similar to self-seed methods. The seed layer in this system is formed by a reaction of converting Zn metal into ZnO. Thus the seed layer is also affected by the quality of Zn metal excluding the effects of the growth solution. This makes understanding the growth character complicated. A series of experiments were designed to understand the growth mechanism of ZnO nanowire arrays in our system. It was found that the growth of ZnO crystal depended on the amount of $NH_3 \cdot H_2O$, reaction temperature, zinc ion concentration, and the zinc plating layer.

In order to show the influence of $NH_3 \cdot H_2O$, different amounts (0.1 g, 1 g, and 2 g) were used, while keeping other parameters unchanged. In 0.1 g $NH_3 \cdot H_2O$, the solution was turbid with some $Zn(OH)_2$ precipitation. When the amount of $NH_3 \cdot H_2O$ was further increased to 1 g, 2 g the solution became clear. The morphologies of the synthesized ZnO nanowire arrays were shown in Figures 3(a) and 3(b), (0.1 g) and Figures 3(c) and 3(d), (2 g). The diameter of ZnO nanowire increased with the increase of $NH_3 \cdot H_2O$ from 100 nm to 220 nm. This may be caused by the fast growth speed of ZnO crystal in higher pH value which resulted from the increase amount of $NH_3 \cdot H_2O$. Moreover, the alignment of ZnO nanowire arrays was also improved with the increase of ammonia addition. This is different with the result reported by Tak and Yong [49]. In their report, the alignment of the nanowire arrays degraded with much more $NH_3 \cdot H_2O$ addition due to the initial overetching and degradation of zinc seed layer in the high pH solution. However, we replaced the thermal-deposited Zn metal layer with electroplating Zn layer in our works. Commonly, the thickness of the electroplating Zn layer, several micrometers, is thicker than the thermal-deposited layer which is only in the scale of nanometer. Thus overetching can be avoided in our system. In addition, their chemical reaction activities are totally different. Compared with the thermal-deposited Zn layer, the electroplated Zn layer is easier to react with the solution due to the intrinsic crystal defects like screw dislocation. The conversion of Zn metal into ZnO reacts as follows [49, 55]:

$$\begin{aligned} Zn + 2OH^- &\longleftrightarrow ZnO_2^{2-} + H_2 \\ ZnO_2^{2-} + H_2O &\longleftrightarrow ZnO_{(s)} + 2OH^- \end{aligned} \tag{1}$$

Zinc metal reacts with hydroxide ions produced by $NH_3 \cdot H_2O$ to produce soluble zincate ions ZnO_2^{2-}. Then the zincate ions react with water and deposit back to the surface of Zn layer to form solid-phase ZnO. With the improvement of the concentration of OH^-, caused by the increase of $NH_3 \cdot H_2O$ addition, reaction will turn to right more fast and produce much more ZnO_2^{2-}, which results in the deposition of much more solid-phase ZnO. Furthermore, a dense layer of ZnO nanoparticles with smaller diameters is formed in higher $NH_3 \cdot H_2O$ concentration. The alignments of the nanowire arrays could be improved by increasing the density of the seed layer [53, 54].

To verify the deduction above, we conducted the experiment etching the Zn plating layer with different amounts of $NH_3 \cdot H_2O$ (0.1 g, 1 g) only at 80°C for 1 h. The obtained surface morphologies of Zn layer were shown in Figure 4(a) (0.1 g) and Figure 4(b) (1 g). The surface in the condition of 0.1 g $NH_3 \cdot H_2O$ was covered by a layer of ZnO particle with much larger diameter than that in 1 g $NH_3 \cdot H_2O$ addition. Meanwhile, the densities were also reduced by decreasing the amount of $NH_3 \cdot H_2O$. Thus, increasing $NH_3 \cdot H_2O$ will result in reducing the diameter of the initial ZnO nanoparticle. By investigating the early stage of the reaction, 30 min, the effects were much more obvious. Figures 4(c) and 4(d) illustrate well-oriented ZnO nanoparticle formed in 30 min when 1 g $NH_3 \cdot H_2O$ was added into the solution. In condition of 0.1 g $NH_3 \cdot H_2O$, as shown in Figures 4(e) and 4(f), a layer of the ZnO nanoparticle was also formed but the orientation is not as good as that in 1 g $NH_3 \cdot H_2O$. As reported by many researchers [56, 57], the orientation of the initial ZnO layer has a strong effect on the alignment of the ZnO nanowire arrays. In our work, the increased amount of $NH_3 \cdot H_2O$ improved the orientation of the initial ZnO layer and then improved the alignments of ZnO nanowire arrays.

The growth of ZnO nanowire arrays was also conducted at different reaction temperatures. We found that the aspect ratio increased (smaller diameters) with the increase of the reaction temperature, but the density decreased. The tips of the nanowire grown at higher temperature also become sharper. In lower temperature, 70°C, shown in Figures 3(e) and 3(f), the nanowire arrays showed average diameter of 160 nm. When heated to 90°C the average diameter becomes smaller, ca. 90 nm. And as clearly shown in Figure 3(f), the tips are sharper and begin to fuse together. As some other researchers have reported [58, 59], the small but highly uniform diameter nanowires tend to bundle and align in the same growth direction and can be described by the phenomena of multiplication growth and the oriented attachment process.

The concentration of the Zinc ions was lowered to further investigate the growth of the ZnO nanowire arrays. When

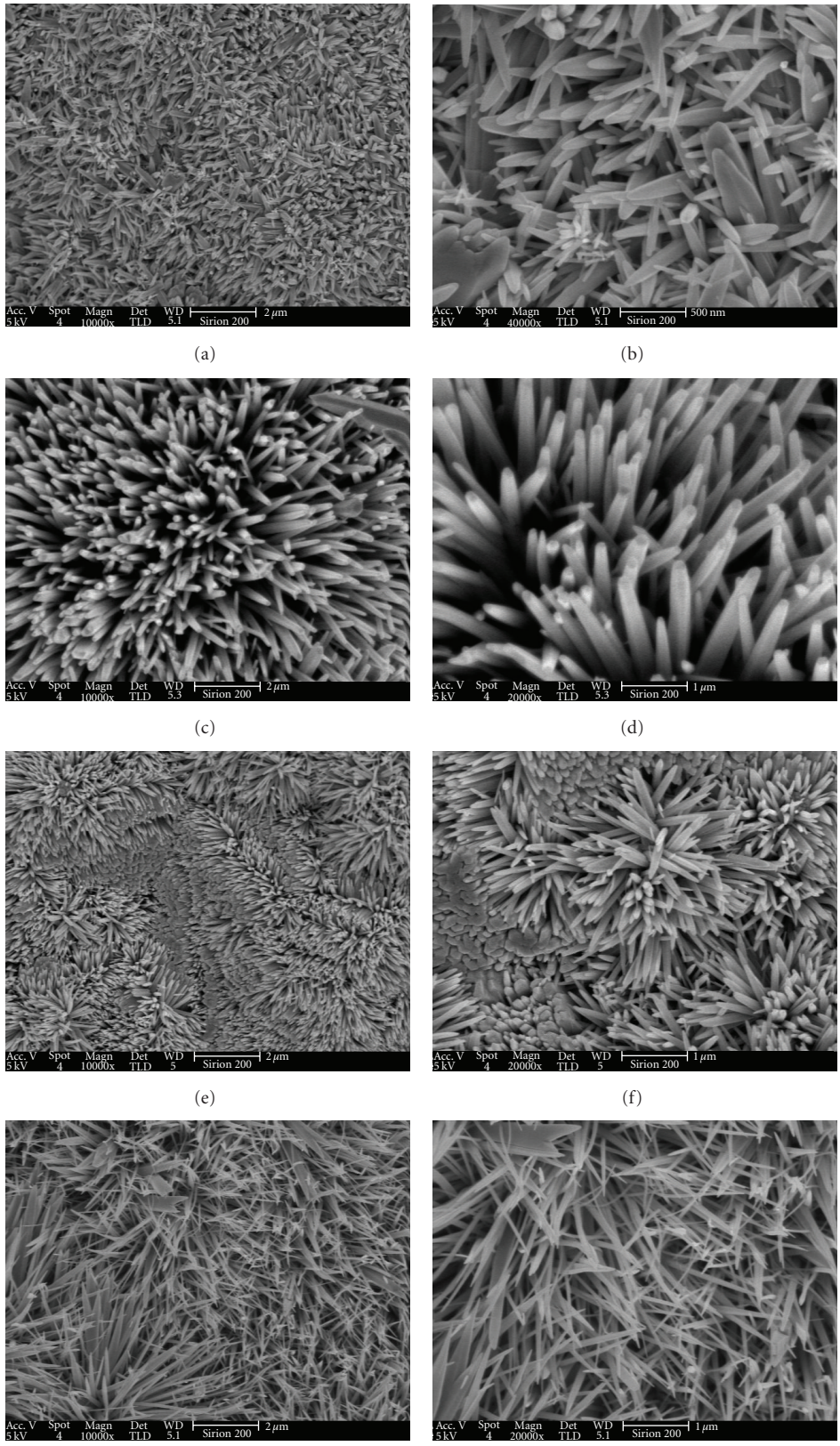

Figure 3: Effect of the amount of the ammonia and temperature, (a, b) 0.1 g, (c, d) 2 g. Effect of temperature (e, f) 70°C (g, h) 90°C.

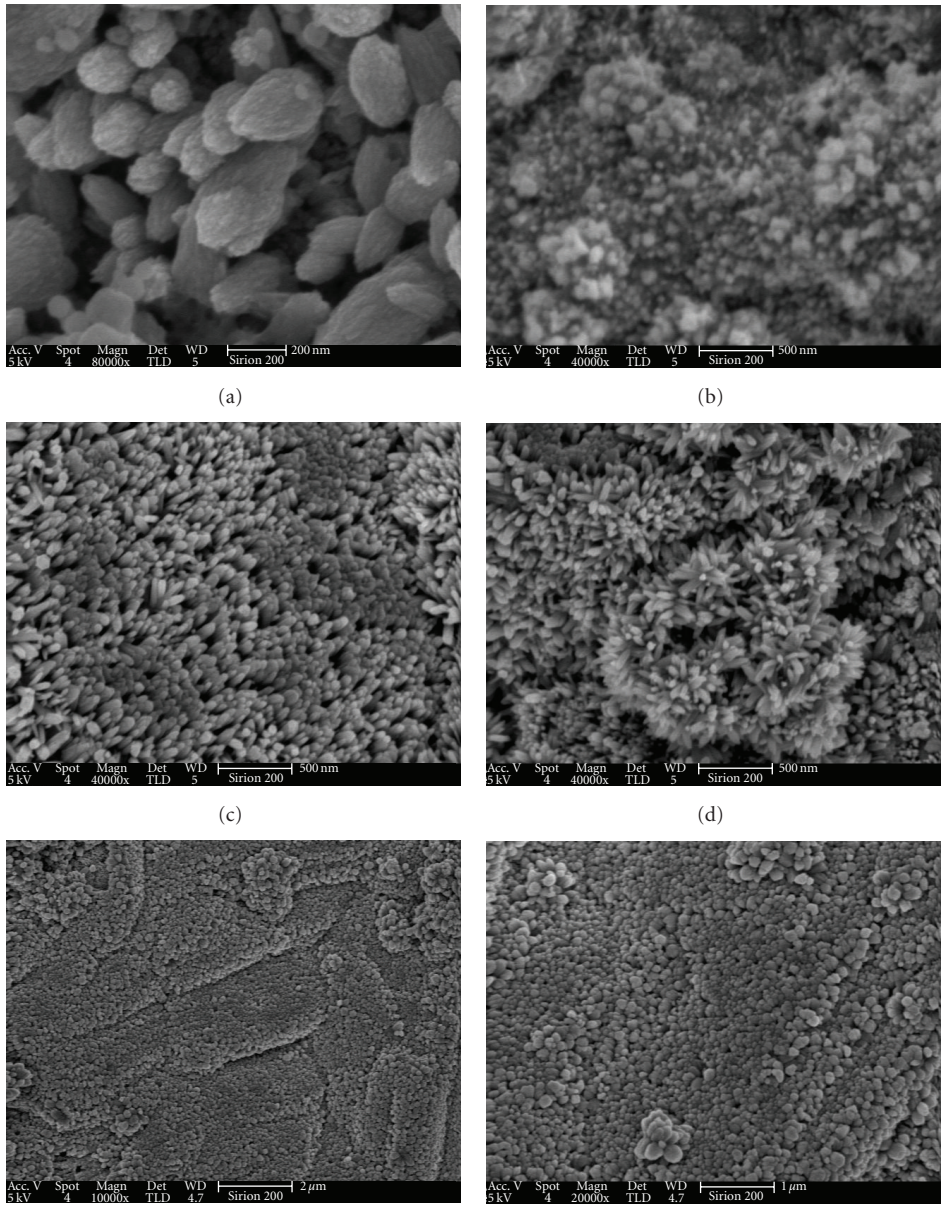

Figure 4: Zn transformed into ZnO in 30 mins, (a, b) only $NH_3.H_2O$, (a) 0.1 g, (b) 1 g, (c, d) 1 g $NH_3.H_2O$, 30 min, (e, f) 0.1 g $NH_3.H_2O$, 30 min.

the zinc ions were decreased to 0.003 M, while keeping $NH_3 \cdot H_2O$ 1 g unchanged, long ZnO nanowire arrays were achieved for 12-hour reaction. The SEM picture of the long ZnO nanowire arrays was shown in Figure 5(a), the inset was enlarged image. The average diameter of the long nanowire arrays was 80 nm and the nanowires fuse together, which was similar to the nanowire arrays synthesized at 90°C. The XRD pattern in Figure 5(b) can be indexed to wurtzite ZnO diffraction pattern (JCPDS Card NO. 36-1451, space group $P6_3mc$). The intensified (101) reflection is caused by the fusion of nanowire arrays. In addition to the ZnO reflection peaks, there also are some peaks indexed to Zn metal retained. We examined the evolution of the long nanowire arrays by different reaction times, 30 min, 1 h, and 6 h. The morphologies of these results were illustrated in Figures 5(c)–5(h). After 30 min of reaction, a dense layer of ZnO nanoparticle, functioned as seed layer, was formed. Figures 5(c) and 5(d) illustrated two typical morphologies of the ZnO nanoparticle. No matter how the different topographies of Zn plating layer presented, the seed layer duplicated the morphologies. When the reaction continued to 1 h, as shown in Figures 5(e) and 5(f), nanowire arrays formed with average diameter of 50 nm. When it was further prolonged to 6 h, the average diameter increased to 60 nm (Figures 5(g) and 5(h)). The diameter increased with the continuing of the reaction and decreased with the lowering of the concentration of Zn^{2+} ions.

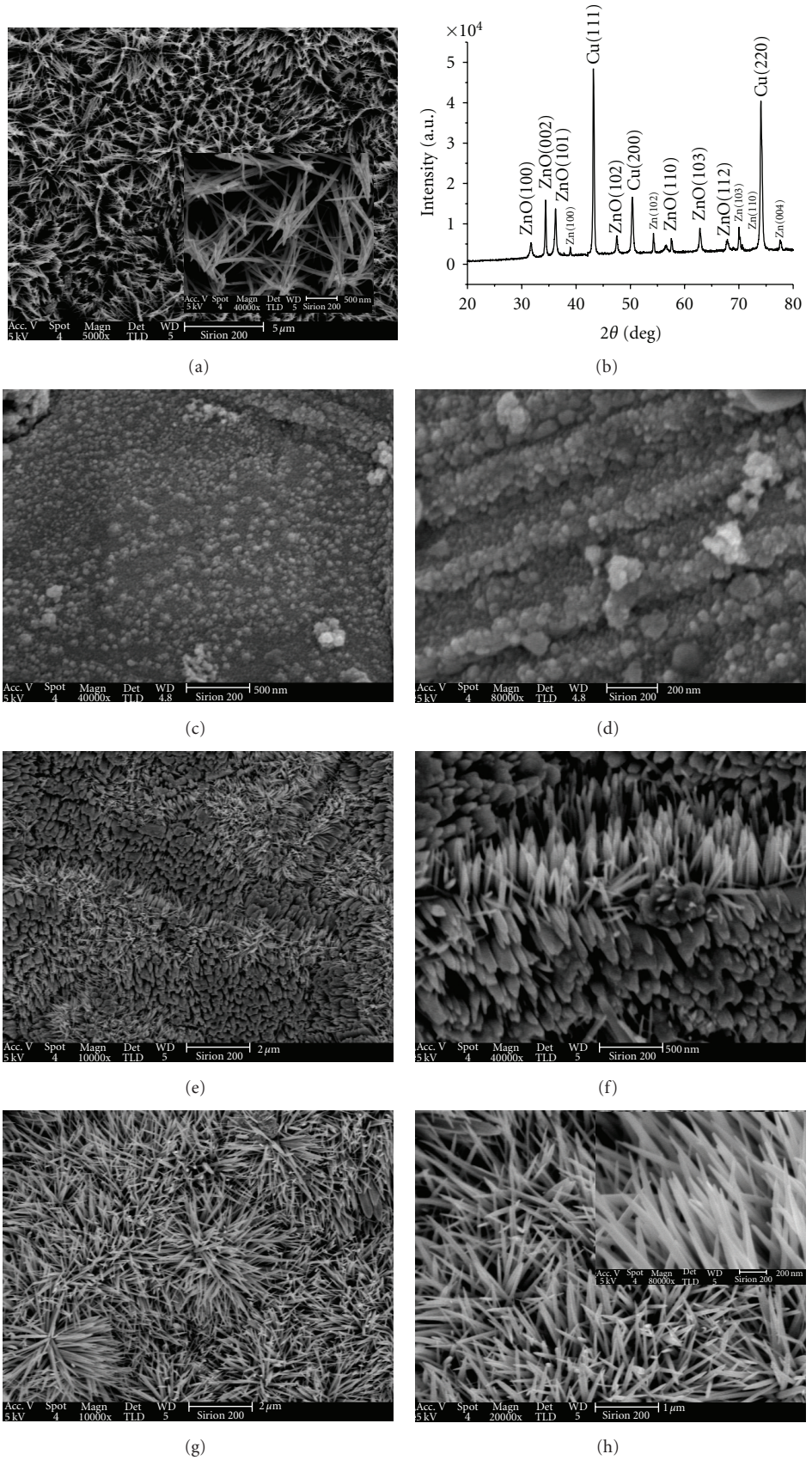

Figure 5: SEM image of long ZnO nanowire arrays (a) 12 h, (c, d) 30 min, (e, f) 1 h, (g, h) 6 h, (b) XRD pattern of long nanowire arrays. The inset of (a) shows enlarged picture with scale bar 500 nm.

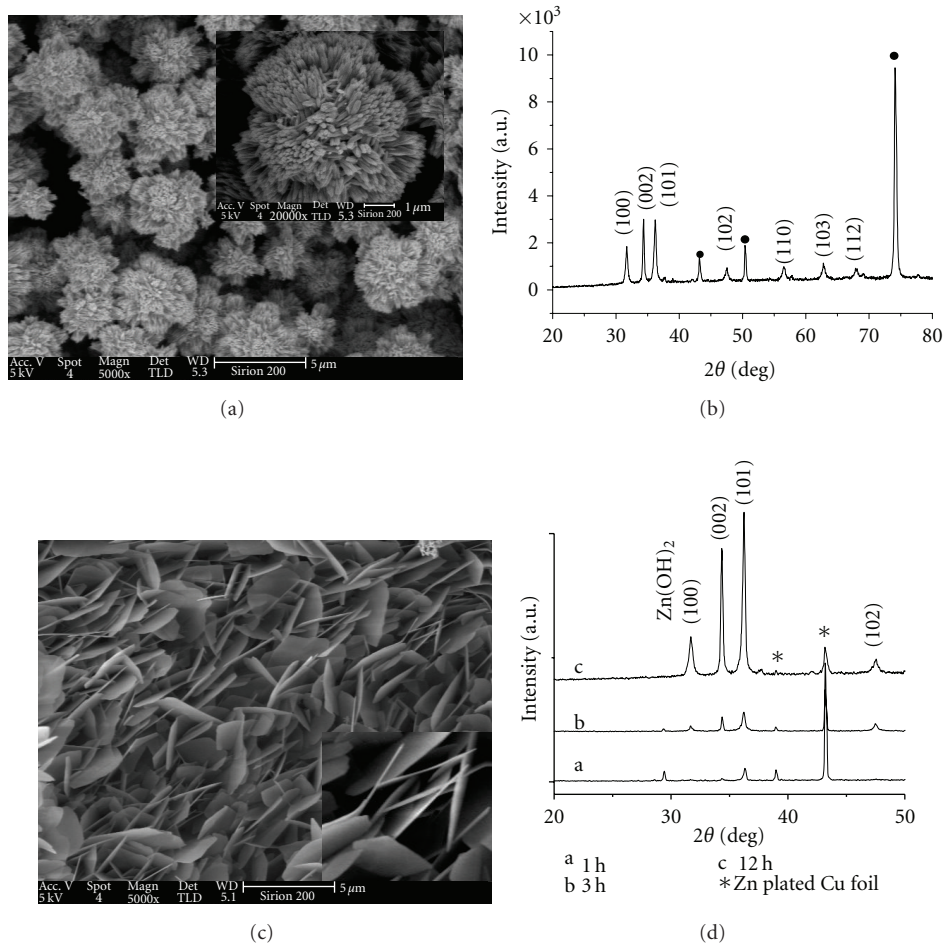

Figure 6: (a) SEM image of flower structure, inset is the image of single flower structure with scale bar 1 μm. (b) XRD pattern of flower structure. (c) SEM image of nanoplate arrays. (d) XRD pattern of nanoplate arrays with time 1 h, 3 h, and 12 h.

Interestingly, two other different morphologies, flower-like structure and nanoplate arrays were achieved in our experiments. We found a white layer deposited on the nonzinc plating side of Cu foil in the solution of 0.1 g $NH_3 \cdot H_2O$ and 0.03 M $Zn(NO_3)_2$ at 80°C. The morphology of this white layer is illustrated in Figure 6(a). A uniform ZnO layer with flower-like structure was observed. As shown in the inset of Figure 6(a), the surface of the flower-like particle was composed of ZnO nanorod arrays. This is a useful structure with high surface area. The corresponding XRD pattern is shown in Figure 6(b). All peaks can be indexed to wurtzite ZnO (JCPDS Card NO. 36-1451, space group $P6_3mc$) except the peaks from the Cu substrates. The (100), (101) reflection are intensified compared with the XRD pattern of ZnO nanowire arrays. Moreover the intensities of (002) and (101) are almost the same, which is like the XRD pattern of other reported ZnO flower-like structures. Generally, homogeneous reaction in the solution and heterogeneous on the substrate happened in the same time. When the amount of $NH_3 \cdot H_2O$ was 0.1 g, the solution was turbid, indicating the formation of $Zn(OH)_2$ precipitations. With the heating of the solution, $Zn(OH)_2$ decomposed to ZnO nuclei in the bulk solution. This process facilitated the growth of ZnO crystal in the solution. As reported by others [60, 61], the growth of ZnO in solution makes it easy to bundle together to form flower-like structure.

In 0.1 g $NH_3 \cdot H_2O$, 0.03 M $Zn(NO_3)_2$ condition, when the temperature increased to 90°C, nanoplate arrays were prepared (Figure 6(c)).The inset is the enlarged image. The thickness of the plate is 50–60 nm, and the average diameters of a single plate are several micrometers. Liu and Zeng [55] also get a hollow ZnO dandelions structure with plate-like building units using Zn metal power as substrates in higher temperature. However, they did not discuss the formation mechanism of the plate like structure. ZnO nanoplate arrays have been reported to be due to the hydrolysis of zinc hydroxide which is usually plate-like. According to the XRD pattern of different growth times (Figure 6(d)1–3), 30 min, 3 h, and 12 h, a reflection at 29.4 degree was observed in the first 30 min stage which is indexed to $Zn(OH)_2$. When the reaction continued, this reflection diminished and reflection peaks of ZnO appeared. Figure 6(d)-3 is the XRD pattern of well-developed ZnO nanoplate arrays. And it can be indexed to the hexagonal wurtzite phase ZnO (JCPDS Card NO.36-1451, space group $P6_3mc$).

The chemical reaction, in our experiments is shown in the following:

$$\begin{aligned} NH_3 \cdot H_2O &\longleftrightarrow NH_4^+ + OH^- \\ Zn^{2+} + 2OH^- &\longleftrightarrow Zn(OH)_{2(s)} \\ Zn^{2+} + 4NH_3 &\longleftrightarrow [Zn(NH_3)_4]^{2+} \\ Zn^{2+} + 4OH^- &\xrightarrow{\Delta} Zn(OH)_4^{2-} \xrightarrow{\Delta} ZnO_{(s)} \end{aligned} \quad (2)$$

When the $NH_3 \cdot H_2O$ was added, it hydrolyzed to NH_4^+ ion and OH^- ion, as shown in (2). The produced OH^- ion reacts with Zn^{2+} ion quickly to form $Zn(OH)_2$ white precipitation (4), and the solution turned turbid. With continued addition of $NH_3 \cdot H_2O$, the solution became clear by the formation of $Zn(NH_3)_4^{2+}$ (5). When the temperature elevated, the (5) turned to left, and the $Zn(NH3)_4^{2+}$ complex decomposed to produce Zn^{2+}. Then $Zn(OH)_4^{2-}$ formed, which served as the basic growth units of ZnO nanoforms, hydrolyzed to $ZnO_{(s)}$ (6). For the growth of ZnO nanowire arrays, the heterogeneous nucleation took place preferentially on the ZnO seed surface due to the reduced nucleation barrier by decreasing the interface energy. In addition, we can get much more understanding of the growth of ZnO nanowire arrays if the crystal habits are considered. Wurtzite ZnO crystal is a polar crystal, exhibiting a positive polar plane that is rich in Zn (0001) and a negative polar plane that is rich in O (000-1). The growth rates of different planes are reported to be V(0001)> V(10-11)> V(1010)> V(000-1). In addition, the negative charged $Zn(OH)_4^{2-}$ complex ions are preferentially adsorbed onto the positive charged (0001) Zn face and subsequently dehydrate and enter into the crystal lattice. The growth rate of the (0001) face is greatly favored, and the more rapid the growth rate, the quicker the disappearance of the basal plane. Thus, nanowire structure with elongated c-axis surrounded by six {10-10} facets is formed. While the growth rates of some {10-11} facets are relatively smaller than those of (0001), and they remained to form needle like tips.

When the amount of $NH_3 \cdot H_2O$ was increased, the stability of $Zn(NH_3)_4^{2+}$ complex ions was also enhanced. As a result, the supersaturation of the solution was lowered. Homogeneous nucleation in the bulk solution was prohibited in low supersaturation, and the heterogeneous nucleation and growth onto the seed layer dominated. As discussed before, the $Zn(OH)_4^{2-}$ growth unit was preferentially attracted onto the (0001) positive charged plane. Monodentate ligand NH_3 can not be efficiently adsorbed onto the neutral {10-10} side faces [62]; thus the increased amount of NH_3could not reduce the diameter. Therefore, the growth rate of the ZnO nanowire was improved in higher amount of $NH_3 \cdot H_2O$, and the diameter of the nanowire was also increased. At higher temperature, the decomposition rate of $Zn(NH_3)_4^{2+}$ complex ions was improved, which further increased the formation of the $Zn(OH)_4^{2-}$ complex ions. Thus the growth along the (0001) direction was improved and the diameter of the nanowire was decreased. When we decreased the concentration of Zn^{2+} ions and kept the amount of $NH_3 \cdot H_2O$ and temperature unchanged, the ratio of Zn^{2+} ions to NH_3 was decreased. This resulted in further decrease in supersaturation of the solution. The homogeneous nucleation was retarded, and the heterogeneous nucleation onto the seeded ZnO crystal was promoted in addition. Also, the critical diffusion of monomers and the subsequent limited growth in the solution of lowered Zn^{2+} ions concentration helped to decrease the diameter of the nanowire. Thus, in the same temperature, when the concentration of Zn^{2+} ions was decreased, the diameter of as-prepared ZnO nanowire was also decreased, and much longer nanowire arrays were achieved, which is similar to the results of Lionel Vayssieres [26].

The room temperature photoluminescence (PL) spectra of the ZnO nanowire arrays, flower-like structure, nanoplate arrays, and long nanowire arrays were measured by using a He-Cd 325 nm wavelength laser as the excitation source, as shown in Figure 7. For the nanowire arrays, Figure 7(a), room temperature PL spectra showed a strong UV emission around 392 nm (3.16 eV) and a broad green emission at ~550 nm (2.25 eV). The PL spectra of flower-like structure exhibited a strong emission around 403 nm (3.07 eV) and a broad green emission at ~550 nm (Figure 7(b)). For the nanoplate arrays, Figure 7(c), a strong UV emission around 383 nm (3.23 eV) and a broad green emission at ~550 nm were observed. The long nanowire arrays, in Figure 7(d), showed an intensive emission around 400 nm (3.09 eV), and the green emission at ~550 nm was relativly weak. Generally, the strong UV emission ranging from 380 to 400 nm is the band-edge emission resulting from the recombination of free excitons, while the green emission centered at about 550 nm is attributed to the singly ionized oxygen vacancy, and the emission results from the radiative recombination of a photogenerated hole with an electron occupying the oxygen vacancy. The shift of the strong UV emission is contributed to an increase in crystal intrinsic defects. Lin et al. [63] have calculated the energy levels of various intrinsic defect centres, such as vacancies of oxygen and zinc, interstitial oxygen and zinc, and antisite oxygen in ZnO. The energy gap between the conduction band (Ec) and the valence band (Ev) is considered to be 3.36 eV. The emission energy of electronic transition from the bottom of the conduction band to the vacancy of zinc (V_{Zn}) level is 3.06 eV, and the emission energy of electronic transition from the bottom of the conduction band to the antisite oxygen (O_{Zn}) level is 2.38 eV. Thus, the shift of UV emission from 383 nm to 403 nm of different ZnO nanostructures indicated different contents of the vacancy of zinc in each nanostructure which was achieved in different growth conditions. In our solution synthesis, the growth units are $[Zn(OH)_4]^{2-}$ produced by the reaction between Zn^{2+} and OH^-, and Zn^{2+} is released from the stabilized $Zn(NH_3)_4^{2+}$ complex ions; OH^- is released from reagent $NH_3 \cdot H_2O$. ZnO is crystallized by continuously adding the O-contained growth units to the as-formed nuclei. The deficiency of Zn^{2+} ion in long ZnO nanowire condition accounts for the vacancy of the zinc. With increasing growth temperature, the release of Zn^{2+} is improved by the decrease of thermostabilization of the $Zn(NH_3)_4^{2+}$ complex ions. Thus, in higher temperature, ZnO nanoplate arrays have less V_{Zn} than that of the flower-like structure which synthesized

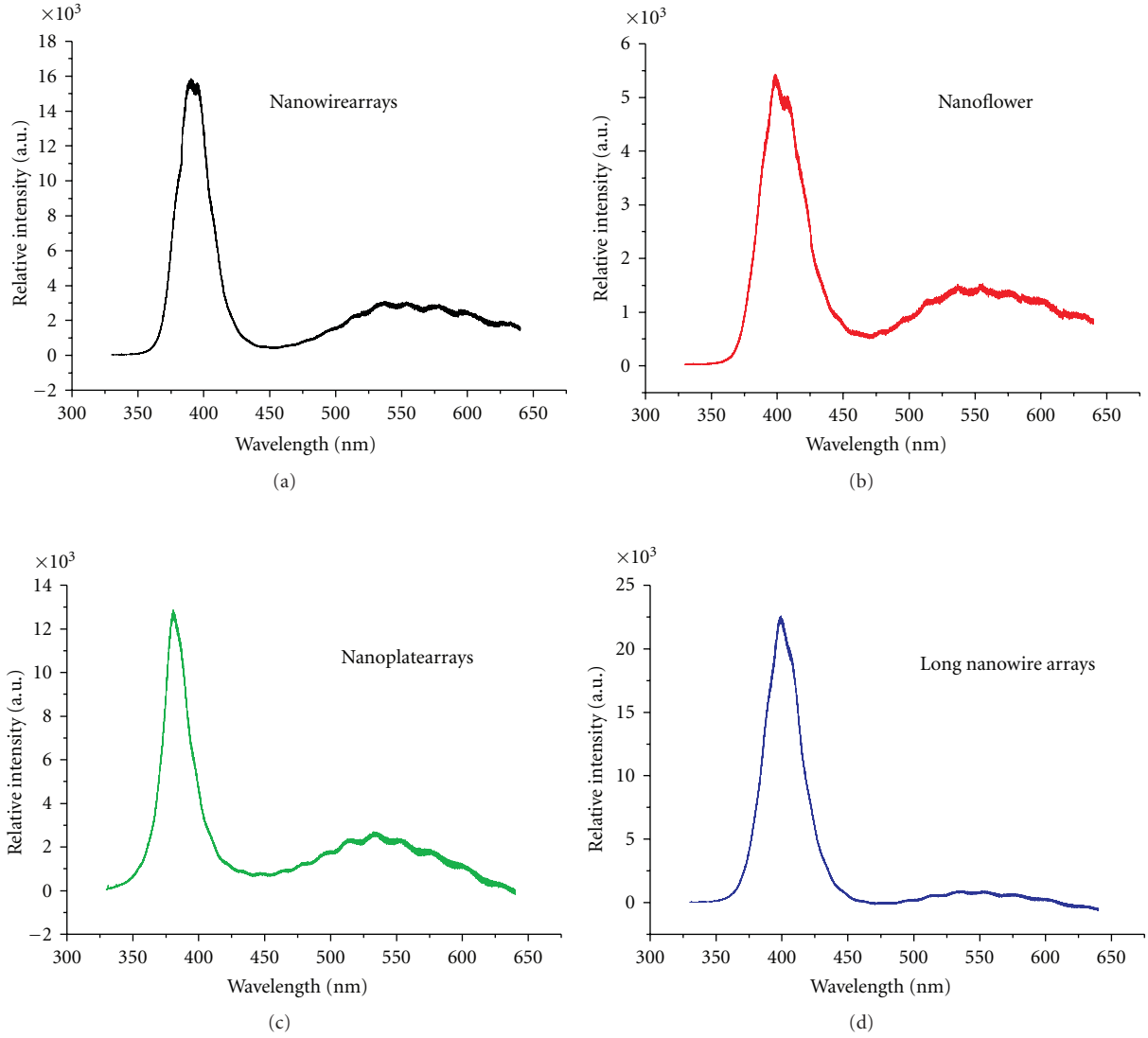

Figure 7: PL spectra of various ZnO nanostructures.

at lower temperature. Therefore, the optical properties can be turned by the growth condition in the solution methods.

4. Conclusion

In conclusion, Zn plating layer on the flexible substrates (copper foil for demonstration here) was successfully applied to prepare ZnO nanostructure arrays via mild solution methods ($Zn(NO_3)_2$/ $NH_3 \cdot H_2O$ solution system) in 70–90°C. Various synthetic conditions were demonstrated to influence the nanostructure arrays. It was found that, by varying the ratio of $NH_3 \cdot H_2O$ to $Zn(NO_3)_2$, the achieved ZnO nanostructure controllably changed from flower-like to nanowire arrays in which the seed layer formation process and diffusion rates of Zn^{2+} ions played important roles. By increasing the growth temperature, or reducing the Zn^{2+} ion concentration, the diameter of ZnO nanowire arrays can also be reduced greatly from 200 nm to 60 nm. It is noted that the amounts of $NH_3 \cdot H_2O$ have great effects on the formation of ZnO seed layer in the initial stage. Dense and orientated seed layers formed in 1 g $NH_3 \cdot H_2O$ are effective for achieving aligned ZnO nanowire arrays. ZnO nanoplate arrays were achieved in 0.03 M $Zn(NO_3)_2$ and 0.1 g $Zn(NO_3)_2$ in 70°C. Moreover, we found that the pattern of ZnO nanowire arrays duplicated the surface morphology of the Zn plating layer which can be changed by controlling the electroplating parameters like electric density. Thus, a new patterning method for ZnO nanowire arrays can be developed by designing the pattern of the Zn plating layer. PL measurement has demonstrated intensive UV exciton luminescence of these ZnO structures which is in the range of 380–403 nm. Therefore, our methods provide an easier and more economic way to produce ZnO nanowire arrays on the flexible conductive substrates and will be applicable to flexible devices like solar cell and gas sensors.

Acknowledgments

The authors thank the financial supports from the National High Technology Research and Development Program of China (no. 2007AA03Z301), the Natural Science Foundations of China (no. 20771032, no. 60806028) and Anhui Province (070414200), and the National Basic Research Program of China (no. 2007CB9-36001).

References

[1] R. F. Service, "Inorganic electronic begin to flex their muscle," *The Science*, vol. 312, no. 5780, pp. 1593–1594, 2006.

[2] R. H. Reuss, B. R. Chalamala, A. Moussessian et al., "Macroelectronics: perspectives on technology and applications," *Proceedings of the IEEE*, vol. 93, no. 7, pp. 1239–1256, 2005.

[3] Z.-Y. Fan, H. Razavi, J.-W. Do et al., "Three-dimensional nanopillar-array photovoltaics on low-cost and flexible substrates," *Nature Materials*, vol. 8, no. 8, pp. 648–653, 2009.

[4] W.-X. Zhang and S.-H. Yang, "In situ fabrication of inorganic nanowire arrays grown from and aligned on metal substrates," *Accounts of Chemical Research*, vol. 42, no. 10, pp. 1617–1627, 2009.

[5] Z. L. Wang, "ZnO nanowire and nanobelt platform for nanotechnology," *Materials Science and Engineering R*, vol. 64, no. 3-4, pp. 33–71, 2009.

[6] Z. L. Wang, "Theme issue: inorganic nanotubes and nanowires," *Journal of Materials Chemistry*, vol. 19, no. 7, pp. 826–827, 2009.

[7] L. Xu, Y.-S. Ding, C.-H. Chen et al., "3D flowerlike α-nickel hydroxide with enhanced electrochemical activity synthesized by microwave-assisted hydrothermal method," *Chemistry of Materials*, vol. 20, no. 1, pp. 308–316, 2008.

[8] M. T. Lloyd, R. P. Prasankumar, M. B. Sinclair, A. C. Mayer, D. C. Olson, and J. W. P. Hsu, "Impact of interfacial polymer morphology on photoexcitation dynamics and device performance in P3HT/ZnO heterojunctions," *Journal of Materials Chemistry*, vol. 19, no. 26, pp. 4609–4614, 2009.

[9] M. Law, L. E. Greene, J. C. Johnson, R. Saykally, and P. Yang, "Nanowire dye-sensitized solar cells," *Nature Materials*, vol. 4, no. 6, pp. 455–459, 2005.

[10] Y. Tak, S. J. Hong, J. S. Lee, and K. Yong, "Fabrication of ZnO/CdS core/shell nanowire arrays for efficient solar energy conversion," *Journal of Materials Chemistry*, vol. 19, no. 33, pp. 5945–5951, 2009.

[11] L. C. Tien, P. W. Sadik, D. P. Norton et al., "Hydrogen sensing at room temperature with Pt-coated ZnO thin films and nanorods," *Applied Physics Letters*, vol. 87, no. 22, Article ID 222106, 3 pages, 2005.

[12] G. Shen, P.-C. Chen, K. Ryu, and C. Zhou, "Devices and chemical sensing applications of metal oxide nanowires," *Journal of Materials Chemistry*, vol. 19, no. 7, pp. 828–839, 2009.

[13] S.-K. Kim and S. B. Lee, "Highly encoded one-dimensional nanostructures for rapid sensing," *Journal of Materials Chemistry*, vol. 19, no. 10, pp. 1381–1389, 2009.

[14] M. H. Huang, S. Mao, H. Feick et al., "Room-temperature ultraviolet nanowire nanolasers," *The Science*, vol. 292, no. 5523, pp. 1897–1899, 2001.

[15] W. I. Park and G.-C. Yi, "Electroluminescence in n-ZnO nanorod arrays vertically grown on p-GaN," *Advanced Materials*, vol. 16, no. 1, pp. 87–90, 2004.

[16] J. W. Stouwdam and R. A. J. Janssen, "Red, green, and blue quantum dot LEDs with solution processable ZnO nanocrystal electron injection layers," *Journal of Materials Chemistry*, vol. 18, no. 16, pp. 1889–1894, 2008.

[17] X. Wang, J. Song, J. Liu, and L. W. Zhong, "Direct-current nanogenerator driven by ultrasonic waves," *The Science*, vol. 316, no. 5821, pp. 102–105, 2007.

[18] X. D. Wang, J. Zhou, C. S. Lao, J. H. Song, N. S. Xu, and Z. L. Wang, "In situ field emission of density-controlled ZnO nanowire arrays," *Advanced Materials*, vol. 19, no. 12, pp. 1627–1631, 2007.

[19] C. Badre, T. Pauporté, M. Turmine, and D. Lincot, "A ZnO nanowire array film with stable highly water-repellent properties," *Nanotechnology*, vol. 18, no. 36, Article ID 365705, 2007.

[20] Z. W. Pan, Z. R. Dai, and Z. L. W. Wang, "Nanobelts of semiconducting oxides," *The Science*, vol. 291, no. 5510, pp. 1947–1949, 2001.

[21] H.-J. Kim, K. Sung, K.-S. An et al., "ZnO nanowhiskers on ZnO nanoparticle-deposited Si(111) by MOCVD," *Journal of Materials Chemistry*, vol. 14, no. 23, pp. 3396–3397, 2004.

[22] M. H. Huang, Y. Wu, H. Feick, N. Tran, E. Weber, and P. Yang, "Catalytic growth of zinc oxide nanowires by vapor transport," *Advanced Materials*, vol. 13, no. 2, pp. 113–116, 2001.

[23] Z. R. Tian, J. A. Voigt, J. Liu et al., "Complex and oriented ZnO nanostructures," *Nature Materials*, vol. 2, no. 12, pp. 821–826, 2003.

[24] L. E. Greene, M. Law, J. Goldberger et al., "Low-temperature wafer-scale production of ZnO nanowire arrays," *Angewandte Chemie International Edition*, vol. 42, no. 26, pp. 3031–3034, 2003.

[25] D. B. Mitzi, "Solution-processed inorganic semiconductors," *Journal of Materials Chemistry*, vol. 14, no. 15, pp. 2355–2365, 2004.

[26] L. Vayssieres, "Growth of arrayed nanorods and nanowires of ZnO from aqueous solutions," *Advanced Materials*, vol. 15, no. 5, pp. 464–466, 2003.

[27] J. Wang and L. Gao, "Wet chemical synthesis of ultralong and straight single-crystalline ZnO nanowires and their excellent UV emission properties," *Journal of Materials Chemistry*, vol. 13, no. 10, pp. 2551–2554, 2003.

[28] Y. Sun, G. M. Fuge, N. A. Fox, D. J. Riley, and M. N. R. Ashfold, "Synthesis of aligned arrays of ultrathin ZnO nanotubes on a Si wafer coated with a thin ZnO film," *Advanced Materials*, vol. 17, no. 20, pp. 2477–2481, 2005.

[29] J. S. Bendall, G. Visimberga, M. Szachowicz et al., "An investigation into the growth conditions and defect states of laminar ZnO nanostructures," *Journal of Materials Chemistry*, vol. 18, no. 43, pp. 5259–5266, 2008.

[30] H. E. Unalan, P. Hiralal, D. Kuo, B. Parekh, G. Amaratunga, and M. Chhowalla, "Flexible organic photovoltaics from zinc oxide nanowires grown on transparent and conducting single walled carbon nanotube thin films," *Journal of Materials Chemistry*, vol. 18, no. 48, pp. 5909–5912, 2008.

[31] Y. H. Tong, Y. C. Liu, L. Dong et al., "Growth of ZnO nanostructures with different morphologies by using hydrothermal technique," *Journal of Physical Chemistry B*, vol. 110, no. 41, pp. 20263–20267, 2006.

[32] L. E. Greene, M. Law, D. H. Tan et al., "General route to vertical ZnO nanowire arrays using textured ZnO seeds," *Nano Letters*, vol. 5, no. 7, pp. 1231–1236, 2005.

[33] D. Pradhan and K. T. Leung, "Controlled growth of two-dimensional and one-dimensional ZnO nanostructures on indium tin oxide coated glass by direct electrodeposition," *Langmuir*, vol. 24, no. 17, pp. 9707–9716, 2008.

[34] C. Lévy-Clément, R. Tena-Zaera, M. A. Ryan, A. Katty, and G. Hodes, "CdSe-sensitized p-CuSCN/nanowire n-ZnO heterojunctions," *Advanced Materials*, vol. 17, no. 12, pp. 1512–1515, 2005.

[35] R. Tena-Zaera, J. Elias, G. Wang, and C. Lévy-Clément, "Role of chloride ions on electrochemical deposition of ZnO nanowire arrays from O_2 reduction," *Journal of Physical Chemistry C*, vol. 111, no. 45, pp. 16706–16711, 2007.

[36] B. Cao, Y. Li, G. Duan, and W. Cai, "Growth of ZnO nanoneedle arrays with strong ultraviolet emissions by an electrochemical deposition method," *Crystal Growth and Design*, vol. 6, no. 5, pp. 1091–1095, 2006.

[37] Y. Sun, D. J. Riley, and M. N. R. Ashfbld, "Mechanism of ZnO nanotube growth by hydrothermal methods on ZnO film-coated Si substrates," *Journal of Physical Chemistry B*, vol. 110, no. 31, pp. 15186–15192, 2006.

[38] X. D. Yan, Z. W. Li, R. Q. Chen, and W. Gao, "Template growth of ZnO nanorods and microrods with controllable densities," *Crystal Growth and Design*, vol. 8, no. 7, pp. 2406–2410, 2008.

[39] J. P. Liu, X. T. Huang, Y. Y. Li et al., "Vertically aligned 1D ZnO nanostructures on bulk alloy substrates: direct solution synthesis, photoluminescence, and field emission," *Journal of Physical Chemistry C*, vol. 111, no. 13, pp. 4990–4997, 2007.

[40] L. Vayssieres, K. Keis, S.-E. Lindquist, and A. Hagfeldt, "Purpose-built anisotropie metal oxide material: 3D highly oriented microrod array of ZnO," *Journal of Physical Chemistry B*, vol. 105, no. 17, pp. 3350–3352, 2001.

[41] L. Vayssieres, "On the design of advanced metal oxide nanomaterials," *International Journal of Nanotechnology*, vol. 1, no. 1-2, pp. 1–41, 2004.

[42] H. Yu, Z. Zhang, M. Han, X. Hao, and F. Zhu, "A general low-temperature route for large-scale fabrication of highly oriented ZnO nanorod/nanotube arrays," *Journal of the American Chemical Society*, vol. 127, no. 8, pp. 2378–2379, 2005.

[43] F. Xu, Z.-Y. Yuan, G.-H. Du et al., "Simple approach to highly oriented ZnO nanowire arrays: large-scale growth, photoluminescence and photocatalytic properties," *Nanotechnology*, vol. 17, no. 2, pp. 588–594, 2006.

[44] J. W. P. Hsu, Z. R. R. Tian, N. C. Simmons, C. M. Matzke, J. A. Voigt, and J. Liu, "Directed spatial organization of zinc oxide nanorods," *Nano Letters*, vol. 5, no. 1, pp. 83–86, 2005.

[45] W. Schwarzacher, "Electrodeposition: a technology for the future," *Electrochemical Society Interface*, vol. 15, no. 1, pp. 32–33, 2006.

[46] M. Wery, J. C. Catonné, and J. Y. Hihn, "Barrel zinc electrodeposition from alkaline solution," *Journal of Applied Electrochemistry*, vol. 30, no. 2, pp. 165–172, 2000.

[47] S.-H. Jung, E. Oh, K.-H. Lee, W. J. Park, and S.-H. Jeong, "A sonochemical method for fabricating aligned ZnO nanorods," *Advanced Materials*, vol. 19, no. 5, pp. 749–753, 2007.

[48] C. H. Lu, L. M. Qi, J. H. Yang, L. Tang, D. Y. Zhang, and J. M. Ma, "Hydrothermal growth of large-scale micropatterned arrays of ultralong ZnO nanowires and nanobelts on zinc substrate," *Chemical Communications*, no. 33, pp. 3551–3553, 2006.

[49] Y. Tak and K. Yong, "Controlled growth of well-aligned ZnO nanorod array using a novel solution method," *Journal of Physical Chemistry B*, vol. 109, no. 41, pp. 19263–19269, 2005.

[50] B. Liu and C. H. Zeng, "Fabrication of ZnO "Dandelions" via a modified Kirkendall process," *Journal of the American Chemical Society*, vol. 126, no. 51, pp. 16744–16746, 2004.

[51] Biddulph, C.; Marzano, M.; Zinc Plaing, Pavco Inc, Cleveland, P 323.

[52] J. B. Baxter, A. M. Walker, K. V. Ommering, and E. S. Aydil, "Synthesis and characterization of ZnO nanowires and their integration into dye-sensitized solar cells," *Nanotechnology*, vol. 17, no. 11, pp. S304–S312, 2006.

[53] J. C. Liu, J. She, S. Z. Deng, J. Chen, and N. S. Xu, "Ultrathin seed-layer for tuning density of ZnO nanowire arrays and their field emission characteristics," *Journal of Physical Chemistry C*, vol. 112, no. 31, pp. 11685–11690, 2008.

[54] J.-I. Hong, J. Bae, Z. L. Wang, and R. L. Snyder, "Room-temperature, texture-controlled growth of ZnO thin films and their application for growing aligned ZnO nanowire arrays," *Nanotechnology*, vol. 20, no. 8, Article ID 085609, 2009.

[55] B. Liu and H. C. Zeng, "Fabrication of ZnO "Dandelions" via a modified Kirkendall process," *Journal of the American Chemical Society*, vol. 126, no. 51, pp. 16744–16746, 2004.

[56] J. Song and S. Lim, "Effect of seed layer on the growth of ZnO nanorods," *Journal of Physical Chemistry C*, vol. 111, no. 2, pp. 596–600, 2007.

[57] R. Ghosh, M. Dutta, and D. Basak, "Self-seeded growth and ultraviolet photoresponse properties of ZnO nanowire arrays," *Applied Physics Letters*, vol. 91, no. 7, Article ID 073108, 3 pages, 2007.

[58] K. Govender, D. S. Boyle, P. B. Kenway, and P. O'Brien, "Understanding the factors that govern the deposition and morphology of thin films of ZnO from aqueous solution?" *Journal of Materials Chemistry*, vol. 14, no. 16, pp. 2575–2591, 2004.

[59] H. Zhang, D. R. Yang, Y. J. Ji, X. Y. Ma, J. Xu, and D. L. Que, "Low temperature synthesis of flowerlike ZnO nanostructures by cetyltrimethylammonium bromide-assisted hydrothermal process," *Journal of Physical Chemistry B*, vol. 108, no. 13, pp. 3955–3958, 2004.

[60] J. Bico, B. Roman, L. Moulin, and A. Boudaoud, "Elastocapillary coalescence in wet hair," *Nature*, vol. 432, no. 7018, p. 690, 2004.

[61] C. Lu, L. M. Qi, J. Yang, L. Tang, D. Zhang, and J. M. Ma, "Hydrothermal growth of large-scale micropatterned arrays of ultralong ZnO nanowires and nanobelts on zinc substrate," *Chemical Communications*, no. 33, pp. 3551–3553, 2006.

[62] M.-S. Mo, D. B. Wang, X. S. Du et al., "Engineering of nanotips in ZnO submicrorods and patterned arrays," *Crystal Growth and Design*, vol. 9, no. 2, pp. 797–802, 2009.

[63] B. X. Lin, Z. X. Fu, and Y. B. Jia, "Green luminescent center in undoped zinc oxide films deposited on silicon substrates," *Applied Physics Letters*, vol. 79, no. 7, pp. 943–945, 2001.